

THE APPLICATION OF A CYLINDRICAL-SPHERICAL FLOATING RING BEARING AS A DEVICE TO CONTROL STABILITY OF TURBOGENERATORS

P.S. Leung and I.A. Craighead
Newcastle Polytechnic
Newcastle upon Tyne, England

T.S. Wilkinson
NEI Parsons Ltd.
Newcastle upon Tyne, England

The development of a new device to control stability of turbogenerators is described in the present study. The device comprises a floating ring installed between the journal and bearing housing of a fluid film bearing. The journal and the inner surface of the ring are cylindrical whilst the outer surface of the ring and bearing surface are spherical providing axial location of the ring and self-alignment of the bearing. The employment of this device would lead to a consistent machine performance. System stability may be controlled by changing a number of bearing and floating ring parameters. This device also offers an additional advantage of having a very low frictional characteristics.

A feasibility study was carried out to investigate the suitability of the new device to turbogenerator applications. Both theoretical analysis and experimental observations were carried out. Initial results suggest that the new floating ring device is a competitive alternative to other conventional arrangements.

NOTATION

C	film clearance
D	diameter
G_θ, G_β	turbulent coefficients
h	film thickness
\bar{M}_1	non-dimensional inner film viscous moment

$$= \frac{C_1}{\mu R_1^3 L (\omega_1 + \omega_2)} M_1$$

\bar{M}_2	non-dimensional outer film viscous moment
-------------	---

$$= \frac{C_2}{\mu R_2^4 \omega_2} M_2$$

N	rotational speed in rev/s
P	pressure

R	radius
Re	Reynolds' number
S ₁	inner film Sommerfeld number
	$= \frac{\mu (N_1 + N_2) L D_1}{W_1} \left(\frac{R_1}{C_1} \right)^2$
S ₂	outer film Sommerfeld number
	$= \frac{\mu N_2 L D_2}{(W_1 + W_2)} \left(\frac{R_2}{C_2} \right)^2$
Sb	bearing Sommerfeld number
	$= \frac{\mu N_1 L D_1}{W_1} \left(\frac{R_1}{C_1 + C_2} \right)^2$
W	loading
Z	co-ordinate in longitudinal direction
α	(ring speed)/(rotor speed)
β	polar co-ordinate in longitudinal direction
γ	(weight of floating ring)/(bearing load)
ϵ	eccentricity ratio
θ	polar co-ordinate in circumferential direction
τ	viscous shear stress
μ	fluid viscosity
ω	rotational speed in rad/s

SUBSCRIPTS

1	inner fluid film or the journal
2	outer fluid film or the ring

1. INTRODUCTION

Modern designs of turbo-machinery usually aim at larger power output, improved efficiency and higher running speed. These design criteria demand an improved bearing performance. In fact, the industry is always seeking for a better bearing design in order to achieve better control on machine performance. The development of a new type of floating ring bearing and its potential application on turbo-generators is described in this paper. The journal and inner surface of the ring are cylindrical whilst the outer surface of the ring and the bearing are spherical providing axial location of the ring and allowing self alignment of the bearing.

The idea of having a floating ring in a fluid film bearing has existed for some time. The conventional floating ring bearing comprises an annular ring with cylindrical surfaces on both sides of the ring. The ring was allowed to move and rotate freely within the space available. This bearing design is known as the plain floating ring bearing. The earliest recorded use of this bearing can be traced back to 1912 where such a bearing was used in Leyland's vehicles [Campbell (1)]. This type of bearing was also used in a Parsons' steam turbine, and in the connecting rod of Bristol aircraft engines in the 1920's [Shaw and Nussdorfer (2)]. Modifications of the basic design also exist. A literature survey of floating ring bearings can

be found in [Leung (3)].

The new bearing design is an attempt to combine different good features found in conventional bearings into a single physical unit. The spherical outer surface of the ring would allow the bearing to tolerate large misalignments. The presence of two fluid films would possibly increase the damping of bearing. It is known that floating ring bearings usually possess low frictional characteristics. The stability of bearing may also be controlled by a variety of bearing and floating ring parameters. The purpose of the present investigation is to verify these assumptions. The behaviour of the cylindrical-spherical floating ring bearing is first analysed. The bearing performance under different working conditions is then examined and compared with those of equivalent conventional bearings. The possibility of applying the new bearing to turbo-machinery is explored through a case study.

2. ANALYSIS

The configuration of the cylindrical-spherical floating ring bearing is illustrated in Fig 1. The inner fluid film supports the external load acting on the journal whilst the outer fluid film is required to support both the external load and the weight of the floating ring. Lubricant is supplied from the central circumferential grooves to the bearing surfaces. Hence, each fluid film may be analysed as having two shorter fluid films with the L/D ratio half the original value. The effective behaviour of each film is the sum of the shorter films.

The steady state solution of the floating ring bearing is mainly based on two equilibrium conditions,

- a) balance of forces: The sum of the hydrodynamic force of the inner film plus the weight of the floating ring should be equal to the hydrodynamic force of the outer film.
- b) balance of frictional moments on the ring: Under steady state operation, the viscous moment acting on the inside surface of the ring should be equal to the viscous moment acting on the outside surface of the ring.

In order to establish the steady state solution of the bearing, it is necessary to calculate the bearing forces of each bearing film and the viscous moments acting at both sides of the ring. The procedure is described as follows,

2.1 The Reynolds' equation and bearing forces

The Reynolds' equation for the cylindrical inner film can be written as follows,

$$\frac{1}{R_1^2} \frac{\partial}{\partial \theta_1} \left(G_{\theta_1} \frac{h_1^3}{\mu} \frac{\partial P_1}{\partial \mu_1} \right) + \frac{\partial}{\partial Z_1} \left(G_{\beta_1} \frac{h_1^3}{\mu} \frac{\partial P_1}{\partial Z_1} \right) = \frac{(\omega_1 + \omega_2)}{2} \frac{\partial h_1}{\partial \theta_1} + \frac{\partial h_1}{\partial t} \quad (1)$$

and for the spherical outer film, the Reynolds' equation is,

$$\begin{aligned}
& \frac{1}{R_2^2} \frac{1}{\cos^2 \beta_2} \frac{\partial}{\partial \theta_2} \left(G_{\theta_2} \frac{h_2^3}{\mu} \frac{\partial P_2}{\partial \theta_2} \right) + \frac{1}{R_2^2} \frac{\partial}{\partial \beta_2} \left(G_{\beta_2} \frac{h_2^3}{\mu} \frac{\partial P_2}{\partial \beta_2} \right) \\
& + \frac{1}{R_2^2} \theta_2 \tan \beta_2 \frac{\partial}{\partial \theta_2} \left(G_{\beta_2} \frac{h_2^3}{\mu} \frac{\partial P_2}{\partial \beta_2} \right) + \frac{1}{R_2^2} \frac{\partial}{\partial \beta_2} \left(G_{\beta_2} \frac{h_2^3}{\mu} \theta_2 \tan \beta_2 \frac{\partial P_2}{\partial \theta_2} \right) \\
& + \frac{1}{R_2^2} \theta_2 \tan \beta_2 \frac{\partial}{\partial \theta_2} \left(G_{\beta_2} \frac{h_2^3}{\mu} \theta_2 \tan \beta_2 \frac{\partial P_2}{\partial \theta_2} \right) = \frac{\omega_2}{2} \frac{\partial h_2}{\partial \theta_2} + \frac{\partial h_2}{\partial t}
\end{aligned} \tag{2}$$

where G_θ and G_β are coefficients dependent on the local Reynolds' number [Constantinescu (4)], and the film thickness can be expressed as follows,

$$h_1 = C_1 (1 + \varepsilon_1 \cos \theta_1) \tag{3}$$

$$h_2 = C_2 (1 + \varepsilon_2 \cos \theta_2 \cos \beta_2) \tag{4}$$

Equations (1) and (2) can be normalised by using selected non-dimensional groups [Craighead (5) and Leung (3)]. For a given inner and outer eccentricity ratio, the equations can then be solved by the finite difference method. Essentially, the pressure distribution of each fluid film is described by a rectangular mesh and the pressure at each nodal point is determined iteratively. Details of the computational scheme can be found in Craighead (5). The bearing forces may then be obtained by integrating the pressure field by a numerical integration method.

2.2 Frictional moments on the ring

The frictional forces acting on the inside and outside surfaces of the ring are dependent on the viscous shear force of the lubricant in each fluid film which is in turn dependent on the relative velocities of the corresponding solid surfaces enclosing the film. From the Navier-Stokes equation, the viscous shear stresses acting on the ring can be written as,

for the inside surface,

$$\tau_1 = Q \left[\frac{h_1}{2R_1} \frac{\partial P_1}{\partial \theta_1} - \frac{\mu}{h_1} (\omega_1 - \omega_2) R_1 \right] \tag{5}$$

and for the outside surface,

$$\tau_2 = Q \left[\frac{h_2}{2 R_2 \cos \beta_2} \frac{\partial P_2}{\partial \theta_2} + \frac{\mu}{h_2} \omega_2 R_2 \cos \beta_2 \right] \tag{6}$$

Where Q is the ratio of turbulent friction to laminar friction, and is dependent on the mean Reynolds' number of each film. In the present study,

$$\begin{aligned}
Q &= 0.039 \text{ Re}^{0.57} && \text{for turbulent flow} \\
Q &= 1 && \text{for laminar flow}
\end{aligned}$$

The frictional moments can then be obtained by integrating the corresponding shear stress so that,

for the inside surface,

$$M_1 = 2 \int_0^{L/2} \int_0^{2\pi} \tau_1 R_1^2 d\theta_1 dZ_1 \quad (7)$$

and for the outside surface,

$$M_2 = 2 \int_0^{\beta_e} \int_0^{2\pi} \tau_2 R_2^3 \cos^2 \beta_2 d\theta_2 d\beta_2 \quad (8)$$

The frictional moments may be obtained in non-dimensional form, from results of the normalised Reynolds' equation. The viscous friction in the cavitation region of the films is also included in the present study [Ruddy (6) and Leung (3)].

2.3 Calculation procedure for the steady state solution

The computational strategy to determine the steady state solution of the bearing is described in this section. From the balance of forces, the ratio of Sommerfeld number for the inner and outer fluid films can be written as,

$$\frac{S_1}{S_2} - \frac{(1 + \alpha)}{\alpha} \left(\frac{R_1}{R_2} \right)^3 \left(\frac{C_2}{C_1} \right)^2 (1 + \gamma) = 0 = G_1 \quad (9)$$

From the balance of frictional moments, the ratio of the non-dimensional moments acting at inside and outside surfaces of the ring can be written as,

$$\frac{\bar{M}_1}{\bar{M}_2} - \frac{\alpha}{(1 + \alpha)} \left(\frac{R_2}{R_1} \right)^4 \left(\frac{C_1}{C_2} \right) \left(\frac{R_1}{L} \right) = 0 = G_2 \quad (10)$$

Equations (9) and (10) determine the relationship between the inner film eccentricity ratio, the outer film eccentricity ratio, and the (ring speed/rotor speed) ratio. For a given value of inner eccentricity ratio, the equations may then be used to search for the outer film eccentricity ratio and the speed ratio. A modified form of the Newton's iteration method [Gerald (7)] was used in this study, as follows,

$$\begin{bmatrix} \epsilon_2 \\ \alpha \end{bmatrix}_{k+1} = \begin{bmatrix} \epsilon_2 \\ \alpha \end{bmatrix}_k - R_f \begin{bmatrix} \frac{\partial G_1}{\partial \epsilon_2} & \frac{\partial G_1}{\partial \alpha} \\ \frac{\partial G_2}{\partial \epsilon_2} & \frac{\partial G_2}{\partial \alpha} \end{bmatrix}_k^{-1} \begin{bmatrix} G_1 \\ G_2 \end{bmatrix}_k \quad (11)$$

where k indicates the state of successive iterations and R_f is the relaxation factor.

The matrix containing the partial derivatives (the Jacobian matrix) is obtained by numerical perturbation of G_1 and G_2 . The steady state solution is then obtained if a specified tolerance is satisfied. When R_f is equal to unity, the usual Newton's iteration method is used. It provides stable iteration for cases with laminar lubricant flow. However, the iteration may sometimes fail to converge if the lubricant flow is assumed turbulent. An under-relaxation factor of value from 0.5 to 0.75 was found satisfactory for all cases with either assumption. The application of the under-relaxation factor for laminar flow condition could reduce the computational time by up to 20% when compared with the case where R_f is equal to unity.

2.4 The dynamic characteristics of the bearing

The dynamic characteristics of the bearing are represented by a set of eight linearised force coefficients so that the bearing forces acting on the journal can be expressed by the following equations,

$$\begin{aligned} F_x &= A_{xx} X + A_{xy} Y + B_{xx} \dot{X} + B_{xy} \dot{Y} \\ F_y &= A_{yx} X + A_{yy} Y + B_{yx} \dot{X} + B_{yy} \dot{Y} \end{aligned} \quad (12)$$

The displacement coefficients, A's, are obtained by perturbing the displacement of the journal centre from its steady state position. The velocity coefficients, B's, are obtained by perturbing the velocity of the journal centre. These coefficients may then be used to study the stability and response characteristics of the bearing applied to different rotor systems.

3. PARAMETRIC INVESTIGATION OF BEARING PERFORMANCE

To ensure good design and reliable service it is necessary to determine the behaviour of the new bearing under different working conditions. In this study, six bearing parameters were investigated. A bearing with typical parameter values was first selected as the reference case. Each parameter was then varied about the reference conditions and any changes in bearing characteristics have been noted. The results are described as follows.

3.1 The clearance ratio (C_2/C_1)

The ratio of the outer film clearance to the inner film clearance was found to be significant in determining many bearing characteristics. Design charts are given in this case as examples. In the present study, it is assumed that the total clearance of the inner and outer films is constant. Variation of C_2/C_1 is achieved by changing the inner film and outer film clearances at the same time.

For a given operating condition, it was found that increasing C_2/C_1 would cause a reduction in inner film eccentricity ratio, but an increase in outer film eccentricity ratio. As a result, the overall bearing eccentricity ratio, which is defined as the ratio of the journal displacement to the total clearance, is reduced (Fig 2). This implies that the load carrying capacity of the bearing is increased by an increase of clearance ratio. The bearing attitude angle, however, is reduced (Fig 3). Increasing the value of C_2/C_1 will also increase the (ring speed)/ (rotor speed) ratio (Fig 4). Consider that the inner film clearance is reduced as C_2/C_1 is increased, the shear force acting at the inside surface of the ring will then be increased. The speed ratio is therefore increased.

The journal frictional loss (usually indicated by the friction factor) is also increased for a similar reason (Fig 5).

The dynamic coefficients of the bearing are shown in Figs 6 and 7. These coefficients are used to calculate the limit of stability [Craighead (5)] of the bearing (Fig 8). The effect of the clearance ratio on the dynamic stability can be divided into two regions : for low Sommerfeld numbers, the stability is reduced by increasing value of the clearance ratio; for high Sommerfeld numbers, increasing the value of the clearance ratio will increase the limit of stability. Large values of clearance ratio is therefore beneficial in high speed or light load operations. The ratio of the (whirl speed)/(rotor speed + ring speed) was found to be about 0.5 as expected (Fig 9) [Orcutt and Ng (8)]. However, it is common to calculate the (whirl speed/rotor speed) for bearings with a single film. For the floating ring bearing, the value of this ratio will be higher than 0.5 and within the range of 0.6 to 0.7 (Fig 10).

3.2 The ratio of the ring radii (R_2/R_1)

The ratio of the ring outside radius to inside radius also affects the performance of the floating ring bearing. For an increasing value of R_2/R_1 , the frictional moment acting at the outside surface of the ring will be increased. This reduces the (ring/rotor) speed ratio and hence reduces the load carrying capacity of the outer film. As a result, the overall load carrying capacity and attitude angle of the bearing is reduced. The frictional power loss, however, is increased because the reduction of ring speed will increase the frictional force acting at the journal surface. In terms of dynamic characteristics, increasing the value of R_2/R_1 increases the limit of stability of the bearing for the range of Sommerfeld Number examined.

3.3 The (L/D_1) ratio

The effects of varying the L/D_1 ratio on the floating ring bearing are similar to those found in conventional bearings. Increasing the value of L/D_1 ratio will cause an increase in load carrying capacity and attitude angle of the bearing. However, for a given Sommerfeld Number, both the speed ratio and friction factor are not seriously affected by the change in L/D_1 ratio. It should be noted that, if the variation of L/D_1 ratio is achieved by simply varying the length of the bearing, a smaller L/D_1 ratio will result in a smaller Sommerfeld number. In this case, reduction of L/D_1 ratio will cause a slight reduction of the speed ratio and a significant reduction in frictional loss. In terms of dynamic behaviour, a reduction of L/D_1 ratio will increase the limit of stability of the bearing. Hence, a bearing with a small value of L/D_1 ratio is often preferred.

3.4 The mean bearing Reynolds' number

There are two fluid films in a floating ring bearing. The Reynolds' numbers are usually different for each film. In order to ensure comparable results, the mean bearing Reynolds' number of the floating ring bearing is defined herein to indicate the Reynolds' number of an equivalent single film bearing. In the present study, the bearing clearance of the single film bearing is equal to the total clearance of the floating ring bearing. The actual Reynolds' number for the inner and outer films is therefore less than the mean bearing Reynolds' number due to the existence of a rotating ring and a smaller clearance for each film.

The effects of increasing the bearing Reynolds' number on the floating ring bearing are quite similar to those found in single film bearings. However, the floating ring bearing is less sensitive to the change of bearing Reynolds' number, as would be expected. Increasing the value of bearing Reynolds' number will increase the load carrying capacity and the attitude angle of the bearing. The frictional loss is also increased as expected. It should be pointed out that the bearing Reynolds' number has a significant effect on the ring speed ratio. The ring speed is dependent on the viscous friction of the fluid films and the bearing Reynolds' number affects the viscous friction considerably. An increase in Reynolds' number will cause an increase in speed ratio. Also, increasing the value of the bearing Reynolds' number reduces the limit of stability of the bearing.

3.5 The supply pressure

The lubricant supply may sometimes be pressurised, for example, to increase the lubricant flow rate. It was found in this study that pressurising the lubricant increased the load carrying capacity and attitude angle of the floating ring bearing. This was achieved at the cost of reducing bearing stability. It is generally known that the existence of a cavitation region in a bearing may have a stabilising effect on the bearing performance. Pressurising the lubricant, however, will reduce the cavitation region of the bearing.

3.6 The weight of the floating ring

The weight of the floating ring is usually small compared with the loading on the bearing (ie. less than 5%), and is neglected in most analyses. The effect of the loading due to the ring was examined in this study. It was found that the weight of the floating ring had very little effect on both the steady state and the limit of stability of the floating ring bearing. The bearing performance was practically unchanged even when the weight of the ring was increased up to 10% of the bearing loading. This result indicates that the weight of the ring may be neglected without significant loss of accuracy. It also allows more flexibility in selecting the ring material without affecting the bearing performance.

4. COMPARISON WITH OTHER BEARINGS

The steady state and dynamic performance of the cylindrical-spherical floating ring bearing have been compared with an equivalent plain floating ring bearing, a conventional cylindrical bearing and an elliptical bearing. In order to ensure comparable results, all bearing parameters such as the L/D_1 ratio, Reynolds' number, C_2/C_1 ratio and R_2/R_1 ratio, where applicable, are kept identical to those of the cylindrical-spherical floating ring bearing. For the single film bearings, the bearing clearance was equal to the total clearance of the inner and outer fluid films of the floating ring bearing. All bearings studied were analysed by the finite difference technique for finite bearings.

It was found that the behaviour of the cylindrical-spherical floating ring bearing is very similar to that found in a plain floating ring bearing. The load carrying capacity of the spherical outer film of the new bearing is slightly lower than that of the cylindrical outer film of the plain bearing [Leung (9)]. Despite some minor differences, the characteristics of the two floating ring bearings are so close that, for practical purposes, the differences may be ignored. The new floating ring bearing, hence, has the advantage over the plain floating ring bearing of being self aligning.

The load carrying capacity of the floating ring bearing was found to be higher than the cylindrical bearing but lower than the elliptical bearing. The separation of a single fluid film into two thinner films is thought to be reasonable for the increase of the load carrying capacity of the floating ring bearing over the cylindrical bearing. However, the frictional power loss of the floating ring bearing, with laminar lubricant flow, is slightly higher than the loss of the cylindrical bearing but very close to that of the elliptical bearing. For similar reasons as above, the reduction of film thickness will increase the viscous friction in the bearing films and hence increase the frictional loss when compared with the cylindrical bearing. The geometry of the elliptical bearing is responsible for the high load carrying capacity and high frictional loss of the bearing.

The real advantage of the floating ring bearing in terms of energy reduction is its ability to reduce film turbulence when compared to a single film bearing. For a given operating condition (ie. a given Sommerfeld Number), the degree of turbulence in the inner and outer films of the floating ring bearing is less than that of an equivalent cylindrical or elliptical bearing, especially with high Reynolds' numbers. As an example, when the bearing Reynolds' number is increased from laminar to about 3000, the power loss of the single film bearings is increased by 3 to 4 times the original value. The power loss of the floating ring bearing, however, is only increased by about 50% of the original value. As a result, the frictional loss of the floating ring bearing is only about 30 to 40% of that of the single film bearings. Potentially, a considerable amount of energy can be saved.

Stability analyses of the bearings with a rigid rotor show that the limit of stability of the floating ring bearing examined is higher than that of the cylindrical bearing but lower than that of the particular elliptical bearing. It should be pointed out that the ellipticity of the elliptical bearing studied is relatively high (ellipticity = 0.4), which makes the bearing more stable. Although the behaviour of the reference floating ring bearing does reflect the general behaviour of this type of bearing, it is not optimised for high stability. More favourable results could be obtained with suitable selection of bearing parameters.

4.1 An alternative means of comparison

The results reported so far were concerned with a floating ring bearing having a total inner and outer film clearance equal to the clearance of the equivalent single film bearing : the total clearance was kept constant even when the $C2/C1$ ratio was varied. However, it is also possible to construct a floating ring bearing with the inner film clearance equal to that of the single film bearing. The inner film clearance can be kept unchanged and variation of $C2/C1$ achieved by varying the size of the outer film clearance. The total film clearance of the floating ring bearing is hence larger than that of the equivalent conventional bearing. Most early studies of the floating ring bearing are, in fact, concerned with this second arrangement. The performance of these two arrangements of the cylindrical-spherical floating ring bearing has also been examined in this study.

The first bearing, in which the total clearance of the bearing was kept constant, was found to have a higher load carrying capacity and higher limit of stability when compared with the second arrangement. However, the frictional loss of the second bearing was lower than that of the first arrangement. Because of the larger total clearance, the lubricant flowrate of the second bearing should be larger than the first bearing. Compared to conventional bearings, the load carrying capacity, frictional loss and limit of stability of the second bearing are all lower than those of the particular cylindrical bearing.

The first arrangement is more favourable when load carrying capacity and dynamic stability are important, which is the case for most turbo-machines. The second arrangement is favourable when frictional losses and lubricant overheating are serious problems.

5. A CASE STUDY WITH A SCALED LP TURBINE ROTOR

The application of the cylindrical-spherical floating ring bearing to turbo-machinery has been examined by a case study. The floating ring bearing was used to support a scaled LP turbine rotor. The dynamic behaviour of the system was examined and the performance of the floating ring bearing has been compared with other bearings.

The scaled flexible rotor system constitutes to part of a long term research programme and is dynamically similar to a steam turbine for a 660 MW power plant [Leung (3)]. The bearing loading of a steam turbine is considered relatively high when compared to a fast speed gas turbine. The rotor was originally supported by a pair of elliptical bearings and the bearing Reynolds' number at operating speed was estimated to be about 3500.

The frictional loss of the cylindrical-spherical floating ring bearing at operating speed was found to be only 27% of the loss for elliptical bearings, and 40% of the loss for cylindrical bearings. Hence, considerable amount of energy could be saved by using the floating ring bearing.

The stability of the rotor system was examined by eigen value analysis [ie. Craighead (5)]. Rigid foundation was first assumed. The real and imaginary parts of the eigen values indicate the stability and the system (damped) natural frequencies. Results of the study showed that the highest threshold speed was achieved when the rotor was supported by the elliptical bearing. The threshold speed was about 1.75 times the operating speed. The floating ring bearing came second. The threshold speed was found to be 1.5 times the operating speed. The threshold speed of the rotor with cylindrical bearing was below the operating speed. The cylindrical bearing would hence be unsuitable for this application. At the operating speed, the equivalent damping ratio for the lowest system frequency was 0.26 for the elliptical bearing, and 0.22 for the floating ring bearing. Despite a lower value of damping ratio, the damping in the floating ring bearing is sufficient to ensure safe and stable operation.

System response to mass unbalance was also investigated. It was found that least force was transmitted through the cylindrical bearing to ground. The elliptical bearing came second whilst the force transmitted through the floating ring bearing was the highest among the bearings examined. This result indicates that more attention is required for the supporting foundation if the floating ring bearing is to be employed. Damped flexible foundations are usually used in modern power plants. Results indicate that the forces transmitted to the ground were reduced by the introduction of a flexible foundation. The differences among the bearings in response analysis were also reduced to be very small.

A limited amount of experiments were performed on a rig (Fig 11) to verify the corresponding analysis. Generally the experimental results confirmed the theoretical results [Leung (3)]. It may be interesting to point out that many earlier investigators reported the difficulty to make the floating ring start to rotate.

In the case of turbogenerators, the machines are usually started by using the oil pumping technique. The floating ring would therefore be lifted up initially by hydrostatic pressure. With careful operations, the ring starting problem could be eliminated in turbogenerator applications.

It is worthwhile to point out that instability problems may not necessarily be recognised during the design stage of a machine. Sometimes, dynamic problems only surface after the machine is commissioned and expensive remedy action is necessary. Since the dynamic properties of the floating ring bearing can be controlled by a variety of parameters, the bearing offers more choices (and hence a better chance) to correct the performance of machine.

The results of this case study suggest that each of the bearings examined offers some advantages over the others. The elliptical bearing is slightly favourable in terms of dynamic characteristics. However, the cylindrical-spherical floating ring bearing offers considerable energy saving and it is self aligning. The dynamic characteristics of the bearing is satisfactory, especially with damped flexible foundations. The overall performance of the cylindrical-spherical floating ring bearing makes it competitive with the elliptical bearing. Despite good response characteristics and simple geometry, the cylindrical bearing is not favourable in this application.

6. CONCLUSIONS

The development of the cylindrical-spherical floating ring bearing is described. With considerations of the ability to handle misalignment, low frictional characteristics, steady state and dynamic properties, the new bearing has shown favourable performance in turbogenerator applications. The development of this bearing is still in its early stage. The present study, however, demonstrates that the new bearing is an alternative and competitive design which is worthy of consideration.

REFERENCES

- 1) Campbell C
Floating bush bearings
Chartered Mechanical Engineers, March 1987, pp 14.
- 2) Shaw M C and Nussdorfer T J
An analysis of the full-floating journal bearing
NACA Report No 866, 1947.
- 3) Leung P S
An investigation of the dynamic behaviour of floating ring bearing systems and their application to turbogenerators
PhD Thesis, Dept of Mechanical Engineering, Newcastle Polytechnic, 1988.
- 4) Constantinescu V N
Basic relationships in turbulent lubrication and their extensions to include thermal effects
Transaction of A.S.M.E., Paper No 72-Lub-16.

- Craighead I A
A study of the dynamics of rotor-bearing systems and related fluid-film bearing characteristics.
PhD Thesis, Dept of Mechanical Engineering, University of Leeds, 1976.
- 6) Ruddy A V
The dynamics of rotor bearing systems with particular reference to the influence of fluid film journal bearings and the modelling of flexible rotors.
PhD Thesis, Dept of Mechanical Eng, University of Leeds, 1973.
 - 7) Gerald C F
Applied numerical analysis.
Addison-Wesley, 1980.
 - 8) Orcutt F K and Ng C W
Steady-state and dynamic properties of journal bearing in laminar and super-laminar flow regimes.
NASA Report CR-733, June 1967.
 - 9) Leung P S, Craighead I A and Wilkinson T S
An analysis of the steady state and dynamic characteristics of a spherical hydrodynamic journal bearing.
Journal of Tribology, A.S.M.E., July 1989, pp 459-467.
 - 10) Leung P S, Craighead I A and Wilkinson T S
An analysis of the steady state and dynamic characteristics of a cylindrical-spherical floating ring bearing.
IMEchE Conference C242, 1988, pp 349-357.
 - 11) Kettleborough C F
Frictional experiments on lightly-loaded fully floating journal bearings.
Australian Journal of Applied Science, 1955, pp 211-220.
 - 12) Hill H C
Slipper bearings and vibration control in small gas turbines.
Transaction of A.S.M.E., 1958, Vol 80, pp 1756-1764.
 - 13) Dworski J
High speed rotor suspension formed by fully floating hydrodynamic radial and thrust bearings.
Transaction of A.S.M.E., Journal of Engineering for Power, 1964, Vol 86.
 - 14) Kahle G W
Analytical and experimental investigation of a full floating journal bearing.
PhD Thesis, University of Illinois, January 1971.
 - 15) Tanaka M and Hori Y
Stability characteristics of floating bush bearings.
ASLE-ASME Joint Lubrication Conference, October 1971.

- 16) Nakagawa E and Hiroshi A
Unbalance vibration of a rotor-bearing system supported by floating ring bearing.
Bulletin of J.S.M.E., March 1973, Vol 16, pp 503-512.
- 17) Nikolajsen J L
The effect of variable viscosity on the stability of plain journal bearings and floating ring journal bearings.
Journal of Lubrication Technology, October 1973, pp 447-1973.
- 18) Li C H and Rohde S M
On the steady state and dynamic performance characteristics of floating ring bearings.
Journal of Lubrication Technology, July 1981, pp 389-397.
- 19) Tondl A
Some problems of rotor dynamics.
Chapman and Hall, 1965.
- 20) Lund J W
Rotor-bearing dynamics design technology part VII : the three lobe bearing and floating ring bearing.
Mechanical Technology Inc., February 1968.
- 21) Howarth R B
A theoretical analysis of the floating pad journal bearing.
Tribology Convention, 1970.
- 22) Chow C Y
Dynamic characteristics and stability of a helical-grooves floating ring bearing.
Transaction of A.S.L.E., April 1983, Vol 27, pp 154-163.

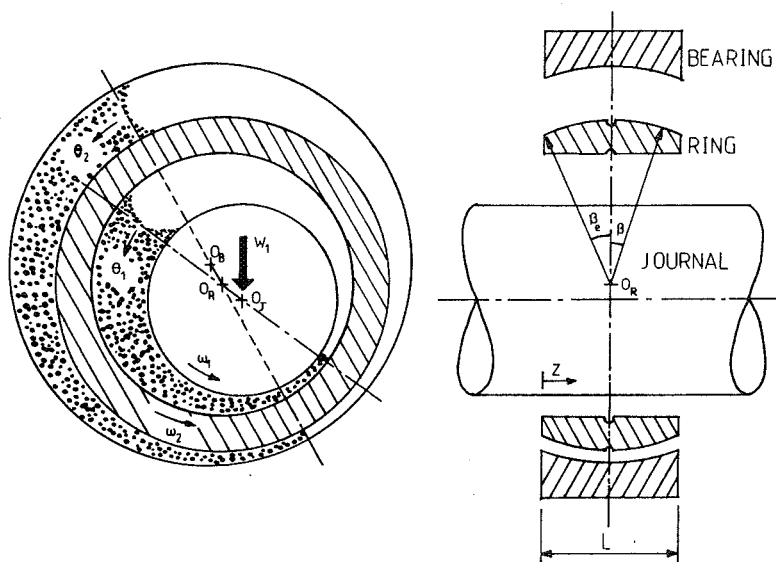


Fig 1 Configuration of the cylindrical-spherical floating ring bearing

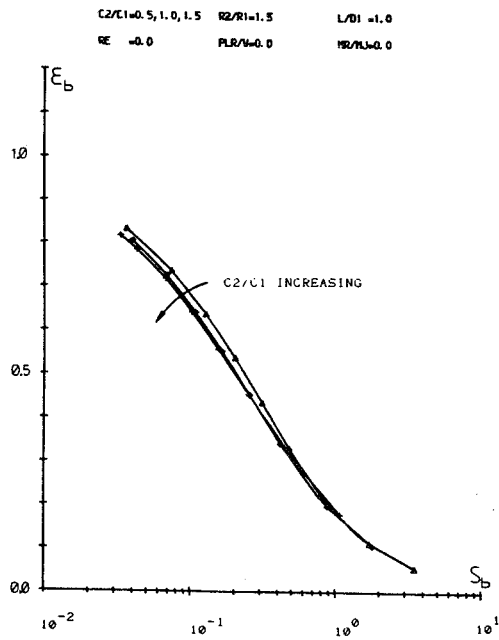


Fig 2 Bearing eccentricity ratio vs Sommerfeld number

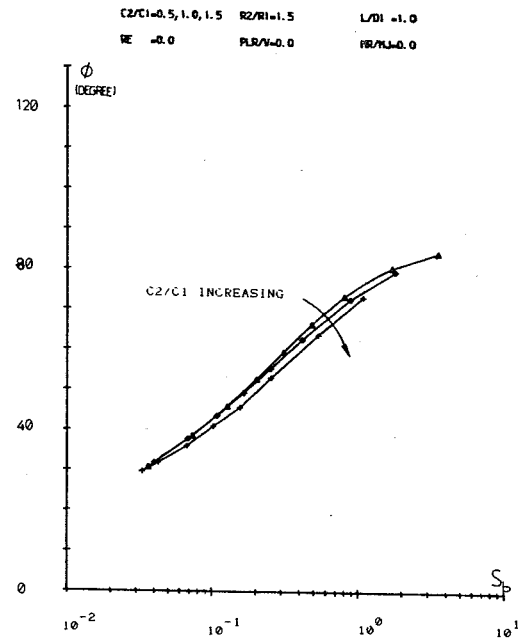


Fig 3 Attitude angle vs Sommerfeld number

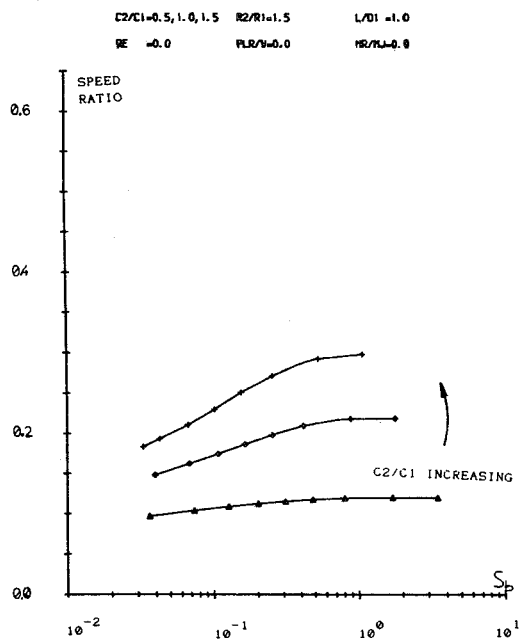


Fig 4 Speed ratio vs Sommerfeld number

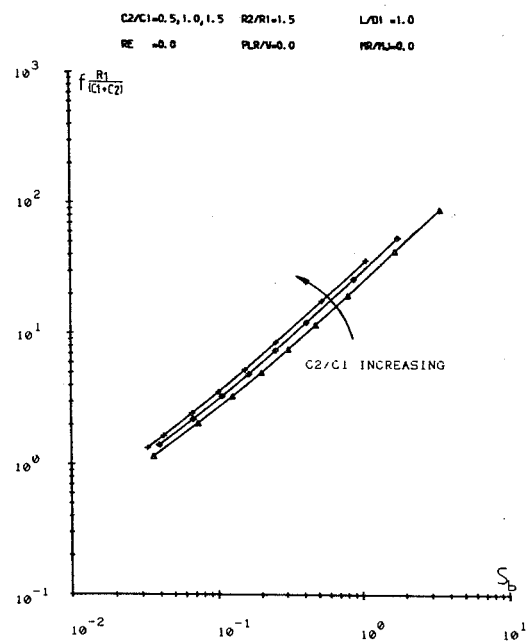


Fig 5 Friction factor vs Sommerfeld number

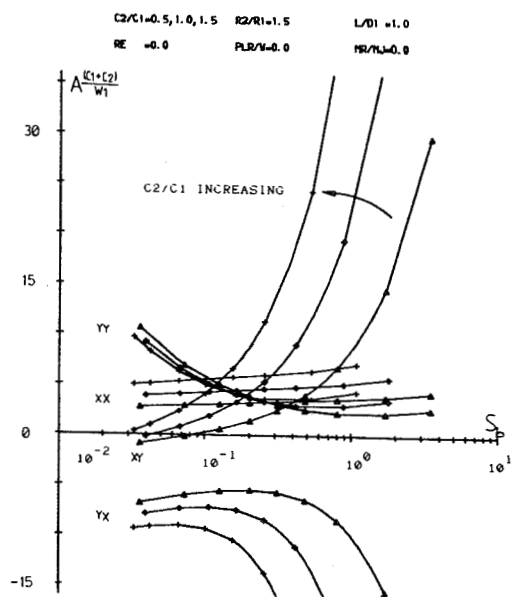


Fig 6 Displacement coefficients vs Sommerfeld number

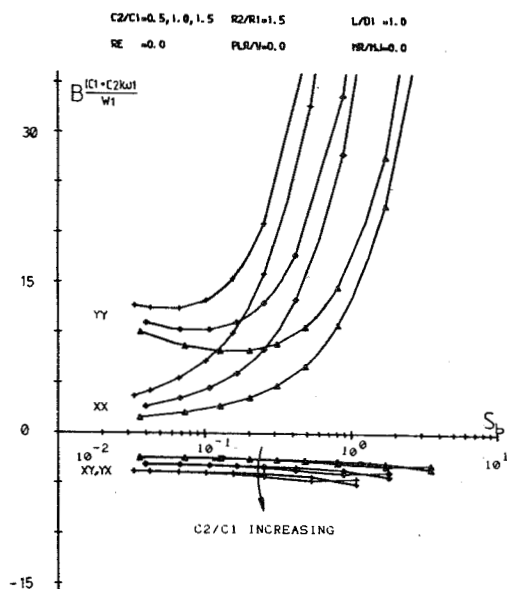


Fig 7 Velocity coefficients vs Sommerfeld number

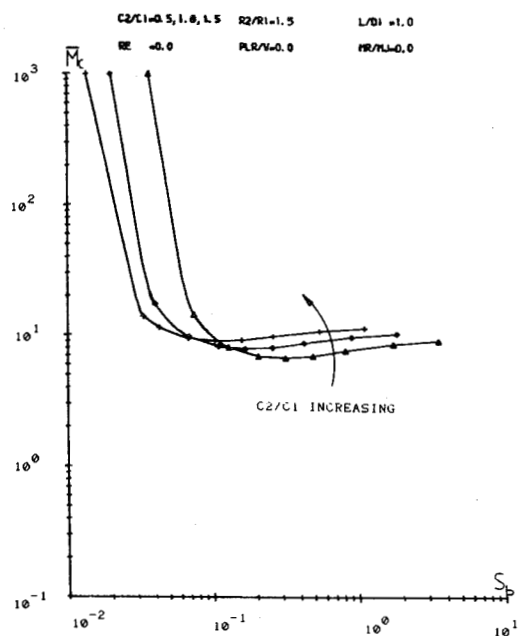


Fig 8 Critical mass vs Sommerfeld number

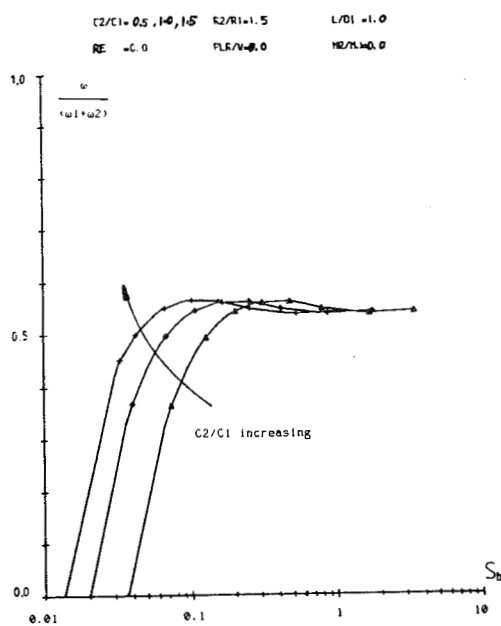


Fig 9 $\omega / (\omega_j + \omega_R)$ vs Sommerfeld number

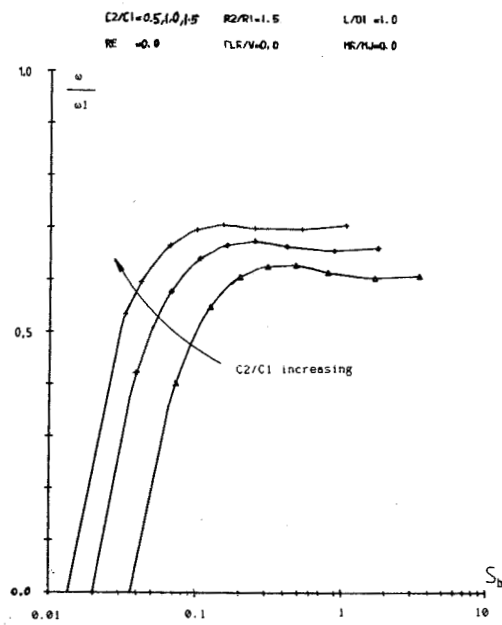


Fig 10 ω/ω_J vs Sommerfeld number

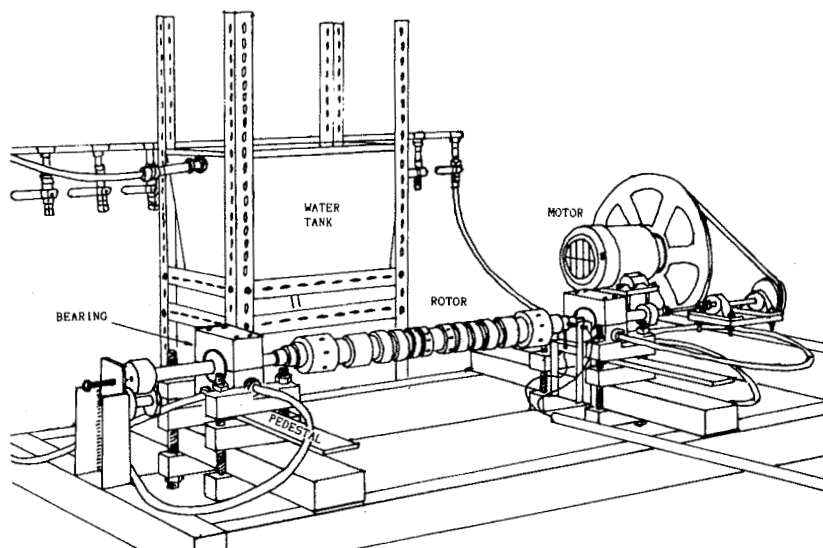


Fig 11 Layout of test rig